

Magnetic order in lightly doped cuprates: Coherent versus incoherent hole quasiparticles and nonmagnetic impurities

Marijana Kirčan^{1,2} and Matthias Vojta²

¹Max-Planck-Institut für Festkörperforschung, Heisenbergstr. 1, 70569 Stuttgart, Germany

²Institut für Theorie der Kondensierten Materie, Universität Karlsruhe, Postfach 6980, 76128 Karlsruhe, Germany

(Received 22 August 2005; published 19 January 2006)

We investigate magnetic properties of lightly doped antiferromagnetic Mott insulators in the presence of nonmagnetic impurities. Within the framework of the t - J model we calculate the doping dependence of the antiferromagnetic order parameter using self-consistent diagrammatic techniques. We show that in the presence of nonmagnetic impurities the antiferromagnetic order is more robust against hole doping in comparison with the impurity-free host, implying that magnetic order can reappear upon Zn doping into lightly hole-doped cuprates. We argue that this is primarily due to the loss of coherence and reduced mobility of the hole quasiparticles caused by impurity scattering. These results are consistent with experimental data on Zn-doped $\text{La}_{2-x}\text{Sr}_x\text{CuO}_4$.

DOI: [10.1103/PhysRevB.73.014516](https://doi.org/10.1103/PhysRevB.73.014516)

PACS number(s): 74.72.-h, 75.50.Ee

I. INTRODUCTION

The undoped parent compounds of the high- T_c superconducting cuprates, such as La_2CuO_4 , are antiferromagnetic (AF) insulators. Upon introducing a small amount of holes, e.g., by substituting La with Sr in La_2CuO_4 , the commensurate long-range order is rapidly suppressed and completely destroyed at few percent of hole doping ($x_c \approx 2\%$ in $\text{La}_{2-x}\text{Sr}_x\text{CuO}_4$).¹ For $2\% < x < 5.5\%$, $\text{La}_{2-x}\text{Sr}_x\text{CuO}_4$ enters a spin-glass phase with incommensurate spin correlations, and finally becomes superconducting for larger x , with only short-range AF correlations in the superconducting state. It is believed that a proper understanding of the magnetism is crucial for a theoretical description of high- T_c cuprates.

On the theoretical side, the suppression of AF order upon hole doping is reasonably well understood.²⁻⁷ Numerous approaches employ effective single-band models with strong correlations to describe the copper oxide planes. The magnetic order, present in the half-filled Néel state, is scrambled by the motion of holes; this leads to heavy hole quasiparticles (so-called magnetic or spin polarons) and to a reduction of the magnetic order parameter, accompanied by a softening of the spin-wave spectrum.²⁻⁴ (A different approach describing the destruction of AF order, based on the idea that holes introduce strongly ferromagnetic frustrating bonds, has been proposed in Refs. 6 and 7.)

Localized impurities provide an interesting tool to investigate bulk properties of strongly correlated systems in general, and high- T_c cuprates in particular. Doping of nonmagnetic impurities (i.e., vacancies) into the parent antiferromagnet,⁸⁻¹⁰ e.g., in $\text{La}_2\text{Cu}_{1-z}\text{Zn}_z\text{O}_4$,¹¹ leads to a gradual suppression of magnetism, with long-range order surviving up to the percolation threshold, $z_p \approx 40.5\%$. One expects that combining hole doping and nonmagnetic impurities would lead to a destruction of the AF order even faster than with hole doping alone. Surprisingly, magnetization measurements on $\text{La}_{2-x}\text{Sr}_x\text{Cu}_{1-z}\text{Zn}_z\text{O}_4$ by Hücker *et al.*¹²

have shown that this is not the case. They found that introducing nonmagnetic Zn impurities in lightly doped $\text{La}_{2-x}\text{Sr}_x\text{CuO}_4$ ($x < 4\%$) causes an initial *increase* of the Néel temperature, T_N , while only an addition of Zn beyond $z \approx 10\%$ leads to a decrease of T_N . Concomitantly, the decrease of T_N with increasing hole doping x is much weaker in Zn-doped compounds. Recently, it has been found that such an impurity-induced reappearance of the AF ordering is even more pronounced in samples with magnetic Ni impurities.¹³

The purpose of the present paper is a theoretical description of the combined effect of mobile holes and static vacancies in lightly doped Mott insulators. We argue below that vacancies primarily prevent the holes from destroying the long-range ordered magnetism; other (purely magnetic) effects are subdominant. Starting from a magnetically ordered state, we consider the influence of mobile holes on the host magnetism in a situation where hole quasiparticles scatter off the static impurities. Technically, we employ a t - J model and the self-consistent Born approximation (SCBA) to account for the interaction between holes and spin waves;^{2,3} the effect of the impurities is treated via a self-consistent T -matrix approach. We show that the destructive effect of holes on the background magnetism is reduced (i) when holes are less mobile or less dispersive and (ii) when holes are less coherent, both changes caused by the addition of nonmagnetic impurities. This results in commensurate antiferromagnetism being more robust against hole doping for impurity-doped host systems compared to clean ones. We obtain detailed magnetization curves as functions of hole and impurity doping, being in good agreement with the available data on $\text{La}_{2-x}\text{Sr}_x\text{Cu}_{1-z}\text{Zn}_z\text{O}_4$. (Incommensurate magnetism, as occurs for hole doping $x > 4\%$, with much smaller ordering temperature, is not the subject of this paper.)

Before describing our theoretical approach, we briefly summarize impurity effects in insulating quantum magnets and in cuprate materials.

A. Impurities in quantum magnets

In a quantum spin system (i.e., a Mott insulator), which can be tuned between an antiferromagnetic and a paramagnetic ground state, the effect of static nonmagnetic impurities (i.e., vacancies) is markedly different in both phases, the origin being the random Berry phases introduced by the doping. As mentioned above, introducing vacancies into the long-range ordered magnet weakens the magnetic order. At small impurity concentrations, this effect can be well captured using linear spin-wave theory.⁹ For a square lattice geometry, long-range magnetism persists up to the percolation threshold¹⁴ z_p ; this has been nicely verified for $\text{La}_2\text{Cu}_{1-z}\text{Zn}_z\text{O}_4$ using neutron scattering.¹¹ The quantum phase transition at z_p displays an interesting interplay of classical percolation physics and quantum effects.^{10,15}

In contrast, removing spins in the quantum paramagnet (which is a valence bond crystal) has been shown to create effective magnetic moments in the vicinity of the dopants.^{16–21} Microscopically, the formation of the moments can be understood as breaking of host valence bonds. The impurity-induced moments are magnetically coupled via the (gapped) host spin excitations and—in the absence of geometric frustration—eventually order at very low temperatures.^{19,20} Thus, at zero temperature the paramagnetic phase of the clean host is replaced by a phase with weak magnetic order through doping with nonmagnetic impurities.

Besides vacancies, magnetic impurities may also be introduced into quantum magnets, either by replacing host ions by ions of different spin (e.g., Cu by Ni), or inserting additional (e.g., out-of-plane) magnetic ions. At small doping, the physics is similar to the one in the case of vacancies, i.e., it is dominated by the low-energy behavior of the impurity moments (random Berry phases), but percolation physics at larger doping is absent.

B. Impurities in cuprates

Impurity effects in cuprate superconductors are diverse, the most prominent being the rapid suppression of superconductivity by in-plane impurities like Zn or Ni substituting for Cu. For hole concentrations in the superconducting regime, it has also been shown that nominally nonmagnetic impurities like Zn or Li induce magnetic moments, which have a staggered spatial structure around the actual impurity site. NMR²² shows that the impurity moments form at temperatures above 400 K, and the formation mechanism is believed to be similar to that in an insulating paramagnet, i.e., breaking of singlet bonds described above. However, impurity-induced magnetic order has not been detected, the reason likely being strong quantum effects (e.g., Kondo screening of the moments) due to the presence of mobile charge carriers. (One exception is magnetic order in Co-doped $\text{YBa}_2\text{Cu}_3\text{O}_{6+\delta}$ (Ref. 23) due to the large spin of Co quantum effects are weaker.) Further effects of Zn and similar impurities in cuprates with larger hole doping include magnetic in-gap states,^{24,25} the broadening of the gapped bulk-spin excitations, possible pinning of charge-density modulations

(stripes), the local modulation of the superconducting order parameter, and large peaks in the density of states close to the Fermi level (as seen, e.g., in scanning tunneling microscopy).

For smaller hole doping (i.e., in the insulating regime), the impurity effects on magnetism and transport have also been studied extensively.^{12,13,26,27} In $\text{La}_{2-x}\text{Sr}_x\text{Cu}_{1-z}\text{Zn}_z\text{O}_4$ with $x \approx 3\%$, codoping with Zn leads to a reappearance of ordered magnetism. The relatively high ordering temperatures suggest that this is *not* just the magnetism of impurity moments as described above for insulating magnets (which would be weak, as in Mg-doped TlCuCl_3 ²⁸). The continuous evolution of the ordering temperature with x and z also hints that the magnetism in the Zn and hole-doped material is smoothly connected to the commensurate antiferromagnetism of the parent compound, i.e., it is neither stripelike nor strongly glassy. (Note that the freezing temperature in the spin-glass state of $\text{La}_{2-x}\text{Sr}_x\text{CuO}_4$ is much below the ordering temperature observed in Refs. 12 and 26. The suppression of glassy behavior upon Zn doping is also consistent with very recent μSR and susceptibility data.²⁹) A natural conclusion is that the Zn impurities primarily “undo” the effect caused by the mobile holes on the commensurate antiferromagnetism. Resistivity measurements in $\text{La}_{2-x}\text{Sr}_x\text{Cu}_{1-z}\text{Zn}_z\text{O}_4$ indicate a decreasing hole mobility with increasing Zn doping. Taken together, we conclude that Zn impurities tend to hinder the coherent motion of holes and thus prevent the magnetic order from being scrambled; this will be the central idea of our approach below. Other effects, namely the generation of effective staggered moments around Zn and vacancy dilution of the magnetism (leading to percolation physics for z close to z_p), are clearly present, but are assumed to be subleading (at least for small impurity concentration).

We note that an interesting dopant in La_2CuO_4 is Li (substituting for Cu); this provides both an extra hole and a vacancy in the CuO plane. Studies^{30,31} of $\text{La}_2\text{Cu}_{1-y}\text{Li}_y\text{O}_4$ have shown that commensurate magnetism survives up to $y=3\%$. Transport data indicate that the holes introduced by Li doping remain localized also for larger y (in contrast to Sr doping). Recent experimental studies show that charge and spin dynamics in $\text{La}_2\text{Cu}_{1-y}\text{Li}_y\text{O}_4$ appear to be glassy over a large range of doping.³¹ Thus, the behavior of $\text{La}_2\text{Cu}_{1-y}\text{Li}_y\text{O}_4$ is different from the one of $\text{La}_{2-x}\text{Sr}_x\text{Cu}_{1-z}\text{Zn}_z\text{O}_4$ with $x=z=y$, the reason clearly being on the quantum chemistry side (e.g., the pinning potentials for holes being different for Li and Zn sites). Reference 32 proposed an antiferromagnetic cluster state arising from Coulomb trapping of holes to explain some of the properties of $\text{La}_2\text{Cu}_{1-y}\text{Li}_y\text{O}_4$, but more theoretical studies are clearly required.

C. Outline

The remainder of the paper is organized as follows. In Sec. II we will introduce the effective model describing the interaction between holes and spin waves. In Sec. III the hole and spin-wave Green's functions will be derived in the framework of the SCBA for the impurity-free system. Effects

of the Zn impurities are discussed in Sec. IV, and Sec. V gives the expressions for magnetic properties within our approach. Finally, numerical results together with a comparison to experimental data are presented in Sec. VI. A discussion concludes the paper.

We note that Korenblit *et al.*³³ have put forward a somewhat different explanation for the experiments of Hücker *et al.*,¹² based on the frustration model.^{6,7} They argued that Zn impurities remove some of the frustrating bonds generated by mobile holes. However, their calculations do not take into account the issue of reduced hole mobility due to impurity doping; we will further comment on their results towards the end of the paper. Impurity effects in cuprates have also been studied within the spin-fermion model.³⁴ The authors do find a recovery of commensurate magnetism in a hole-doped situation upon adding impurities; however, the simplifications within the spin-fermion model (e.g., the absence of quantum spin waves) preclude a comparison with experiments.

II. THE EFFECTIVE HAMILTONIAN

In the following two sections we establish notation and—to keep the paper self-contained—summarize the magnetic polaron model together with its SCBA treatment in the impurity-free situation, following Refs. 2, 3, and 35.

We start from the standard t - J model on a square lattice, $H=H_t+H_J$, and employ a representation using slave-fermion operators f_i for spinless holes and Holstein-Primakoff bosons b_i for spin flips away from the Néel-ordered reference. This gives^{2,36,37}

$$H_t = -t \sum_{\langle i,j \rangle} f_i^\dagger f_j (b_j + b_j^\dagger) - t' \sum_{\langle\langle i,j \rangle\rangle} f_i^\dagger f_j + \text{h.c.}, \quad (1)$$

$$H_J = \frac{J}{2} \sum_{\langle i,j \rangle} (b_i^\dagger b_i + b_j^\dagger b_j + b_i b_j + b_i^\dagger b_j^\dagger) \quad (2)$$

in standard notation. The first kinetic term in (1) describes processes in which holes hop from one to the neighboring site creating or annihilating spin waves; the next-neighbor hopping term t' is allowed for direct hole motion within one sublattice (an additional term of the form $f_i^\dagger f_j b_j b_i^\dagger$ is neglected). Values of $t/J=3-5$, $t'/t=-0.1$ to -0.2 are relevant for cuprate materials. In general, the Heisenberg term (2) contains an additional factor $f_i^\dagger f_i f_j^\dagger f_j$ which accounts for the loss of magnetic energy due to the hole doping. On the mean-field level we have $f_i^\dagger f_i = 1 - f_i^\dagger f_i = 1 - \delta$, where δ is the hole concentration. Consequently, the AF exchange coupling is renormalized according to $J \rightarrow (1 - \delta)^2 J$, but for small hole doping we can neglect this effect.

Fourier transforms of the $b(f)$ are defined in the reduced (magnetic) Brillouin zone, leading to $b_q^A, b_q^B (f_k^A, f_k^B)$ for the two sublattices A and B . The spin-wave part is diagonalized using a Bogoliubov transformation, introducing new bosonic operators for spin waves, α_q and β_q , with $b_q^A = u_q \alpha_q + v_q \beta_{-q}^\dagger$ and $b_q^B = v_q \alpha_q + u_q \beta_{-q}^\dagger$. The usual Bogoliubov parameters are given by

$$u_q = \left[\frac{1 + \kappa_q}{2\kappa_q} \right]^{1/2}, \quad v_q = -\text{sgn}(\gamma_q) \left[\frac{1 - \kappa_q}{2\kappa_q} \right]^{1/2}, \quad (3)$$

with $\gamma_q = (\cos q_x + \cos q_y)/2$ and $\kappa_q = (1 - \gamma_q^2)^{1/2}$. Substituting the new operators α_q, β_q into the Hamiltonian we arrive at the following so-called spin-polaron model:

$$H_t = \frac{zt}{\sqrt{N}} \sum_{\mathbf{q}, \mathbf{k}} [V(\mathbf{q}, \mathbf{k}) f_{\mathbf{k}}^{A\dagger} f_{\mathbf{k}-\mathbf{q}}^B \alpha_{\mathbf{q}} + V(-\mathbf{q}, \mathbf{k} - \mathbf{q}) f_{\mathbf{k}}^{A\dagger} f_{\mathbf{k}-\mathbf{q}}^B \beta_{-\mathbf{q}}^\dagger + \text{h.c.}] + t' \sum_{\mathbf{k}} (f_{\mathbf{k}}^{A\dagger} f_{\mathbf{k}}^A + f_{\mathbf{k}}^{B\dagger} f_{\mathbf{k}}^B),$$

$$H_J = \sum_{\mathbf{q}} \omega_{\mathbf{q}}^0 (\alpha_{\mathbf{q}}^\dagger \alpha_{\mathbf{q}} + \beta_{\mathbf{q}}^\dagger \beta_{\mathbf{q}}). \quad (4)$$

Here, N is the number of sites in each sublattice, and the coordination number is $z=4$. All sums run over the magnetic Brillouin zone. The bare spin-wave energy is $\omega_{\mathbf{q}}^0 = (zJ/2)\kappa_{\mathbf{q}}$. The interaction vertex between holes and spin waves is given by $V(\mathbf{q}, \mathbf{k}) = u_{\mathbf{q}} \gamma_{\mathbf{k}-\mathbf{q}} + v_{\mathbf{q}} \gamma_{\mathbf{k}}$ and vanishes for $\mathbf{q}=0$ or $\mathbf{q}=(\pi, \pi)$. As a consequence, not only the coupling between holes and long-wavelength spin fluctuations is important but also the coupling to short-wavelength spin fluctuations.

III. GREEN'S FUNCTIONS AND BORN APPROXIMATION

The hole Green's function in the absence of impurities is defined by $\mathcal{G}_{\mu\nu}(\tau, \mathbf{k}) = -\langle T_{\tau} f_{\mathbf{k}}^{\mu}(\tau) f_{\mathbf{k}}^{\nu\dagger}(0) \rangle$, $\mu, \nu = A, B$, with the Fourier transform $\mathcal{G}_{\mu\nu}(i\nu_n, \mathbf{k}) = \int_0^{\beta} d\tau \mathcal{G}_{\mu\nu}(\tau, \mathbf{k}) e^{i\nu_n \tau}$, where $\nu_n = (2n+1)\pi T$ represents fermionic Matsubara frequencies. The spin-wave Green's function acquires the matrix form

$$\underline{\mathcal{D}}(\tau, \mathbf{q}) = \begin{bmatrix} -\langle T_{\tau} \alpha_{\mathbf{q}}(\tau) \alpha_{\mathbf{q}}^\dagger(0) \rangle & -\langle T_{\tau} \alpha_{\mathbf{q}}(\tau) \beta_{-\mathbf{q}}(0) \rangle \\ -\langle T_{\tau} \beta_{-\mathbf{q}}^\dagger(\tau) \alpha_{\mathbf{q}}^\dagger(0) \rangle & -\langle T_{\tau} \beta_{-\mathbf{q}}^\dagger(\tau) \beta_{-\mathbf{q}}(0) \rangle \end{bmatrix}.$$

The unperturbed spin-wave propagator is

$$\underline{\mathcal{D}}_0^{-1}(i\omega_n, \mathbf{q}) = \begin{bmatrix} i\omega_n - \omega_{\mathbf{q}}^0 & 0 \\ 0 & -i\omega_n - \omega_{\mathbf{q}}^0 \end{bmatrix}, \quad (5)$$

where $\omega_n = 2\pi nT$. Introducing a self-energy matrix $\underline{\Sigma}(i\omega_n, \mathbf{q})$, the solution of the Dyson equation reads

$$\underline{\mathcal{D}}(i\omega_n, \mathbf{q}) = \frac{1}{d(i\omega_n, \mathbf{q})} \begin{bmatrix} i\omega_n + \omega_{\mathbf{q}}^0 + \Sigma_{22}(i\omega_n, \mathbf{q}) & -\Sigma_{12}(i\omega_n, \mathbf{q}) \\ -\Sigma_{21}(i\omega_n, \mathbf{q}) & -i\omega_n + \omega_{\mathbf{q}}^0 + \Sigma_{11}(i\omega_n, \mathbf{q}) \end{bmatrix}, \quad (6)$$

where

$$d(i\omega_n, \mathbf{q}) = [i\omega_n + \omega_{\mathbf{q}}^0 + \Sigma_{22}(i\omega_n, \mathbf{q})][i\omega_n - \omega_{\mathbf{q}}^0 - \Sigma_{11}(i\omega_n, \mathbf{q})] + \Sigma_{12}(i\omega_n, \mathbf{q})\Sigma_{21}(i\omega_n, \mathbf{q}). \quad (7)$$

The definition of the spin-wave propagators dictates that $\Sigma_{22}(i\omega_n, \mathbf{q}) = \Sigma_{11}(-i\omega_n, -\mathbf{q})$ and $\Sigma_{12}(i\omega_n, \mathbf{q}) = \Sigma_{21}(i\omega_n, \mathbf{q})$.

A. Spin-wave self-energies

The spin-wave self-energies, $\Sigma_{11}(i\omega_n, \mathbf{q})$ and $\Sigma_{12}(i\omega_n, \mathbf{q})$, are calculated in the spirit of SCBA,³⁷ i.e., using the leading (bubble) diagram describing the decay of the spin fluctuations into a particle-hole pair with the *full* hole propagators, see, e.g., Fig. 1 of Ref. 2. This approximation amounts to a summation of an infinite class of noncrossing diagrams; vertex corrections can be shown to be small for small doping³⁸ and will be neglected. Explicitly, the self-energies are given by

$$\Sigma_{11}(i\omega_n, \mathbf{q}) = (zt)^2 \frac{1}{\beta} \sum_{i\nu_n} \frac{1}{N} \sum_{\mathbf{k}} [V(\mathbf{q}, \mathbf{k})]^2 \mathcal{G}_{AA}(i\omega_n + i\nu_n, \mathbf{k}) \times \mathcal{G}_{BB}(i\nu_n, \mathbf{k} - \mathbf{q}), \quad (8)$$

$$\Sigma_{12}(i\omega_n, \mathbf{q}) = (zt)^2 \frac{1}{\beta} \sum_{i\nu_n} \frac{1}{N} \sum_{\mathbf{k}} V(\mathbf{q}, \mathbf{k}) V(-\mathbf{q}, \mathbf{k} - \mathbf{q}) \times \mathcal{G}_{AA}(i\omega_n + i\nu_n, \mathbf{k}) \mathcal{G}_{BB}(i\nu_n, \mathbf{k} - \mathbf{q}). \quad (9)$$

For simplicity and as in Ref. 3, in our numerics we will not perform a fully self-consistent calculation for the hole propagators, but instead use a trial form for the hole spectral density (derived from the SCBA solution of the single-hole problem) together with a rigid-band approximation. (A fully self-consistent SCBA calculation at finite hole concentration has been performed in Ref. 38; it shows that at small hole concentrations the hole spectrum changes little with doping, i.e., the rigid-band picture is reliable.)

B. Hole spectrum

The single-hole problem in the t - J model has been studied extensively using various techniques, including the SCBA within the spin-polaron model sketched above.^{36,39,40} It has been established that the spectral function for a single hole consists of a well-defined peak at low energies, $\rho_{\text{coh}}(\omega, \mathbf{k})$, which corresponds to the coherent motion of the dressed hole quasiparticle, and a broad incoherent part at higher energies,

$$\rho(\omega, \mathbf{k}) = \rho_{\text{coh}}(\omega, \mathbf{k}) + \rho_{\text{incoh}}(\omega, \mathbf{k}). \quad (10)$$

The coherent hole motion arises mainly from a combination of hopping and spin-flip processes and results in a narrow quasiparticle dispersion, $\varepsilon_{\mathbf{k}}$, with a bandwidth of order $2J$ and a dispersion minimum at momenta $\mathbf{k}_{\text{min}} = (\pm\pi/2, \pm\pi/2)$. The quasiparticle weight, Z_0 , is reduced from unity due to the dressing of the hole with spin fluctuation and scales with J/t in the physically relevant parameter regime. Therefore, for the coherent part we use^{2,3}

$$\rho_{\text{coh}}(\omega, \mathbf{k}) = Z_0 \delta(\omega - \varepsilon_{\mathbf{k}}) \Theta(2J - \varepsilon_{\mathbf{k}}), \quad (11)$$

with the dispersion $\varepsilon_{\mathbf{k}} = J(\cos^2 k_x + \cos^2 k_y)$. We have assumed that near the minima the dispersion is isotropic and can be approximated with $\varepsilon_{\mathbf{k}} \approx \bar{k}^2 / (2m_{\text{eff}})$, where \bar{k} measures the distance from the \mathbf{k}_{min} . Consequently, the effective mass of the hole scales as $m_{\text{eff}}^{-1} = 2J$. Here a remark is in order: In the t - J model without next-neighbor hopping, $t' = 0$, the dispersion near \mathbf{k}_{min} is known to be anisotropic, i.e., rather flat along the $(0, \pi) - (\pi, 0)$ direction.⁴¹ However, photoemission results of $\text{Sr}_2\text{CuO}_2\text{Cl}_2$ indicate an almost isotropic dispersion;⁴² on the level of the t - J model a t' term is needed to capture this physics.⁴³ Later on, it has been shown that a t - t' - J model reproduces salient photoemission features of different cuprate families.⁴⁴ Therefore, we employ an isotropic dispersion in the following; we have also performed a few calculations with an anisotropic dispersion appropriate for $t' = 0$, leading to qualitatively similar results (the δ_c in Fig. 1 below changes by less than 10%).

The incoherent part of the spectrum arises from hole hopping inside the spin-polaron (or spin-bag) quasiparticle, with the characteristic energy scale t . A reasonable approximation is a momentum-independent constant,

$$\rho_{\text{incoh}}(\omega) = \frac{1 - Z_0}{W} \Theta(\omega - 2J) \Theta(W + 2J - \omega), \quad (12)$$

where $W = 2zt$ is the incoherent bandwidth.

Within a rigid-band approximation, the hole chemical potential $\mu(\delta)$ is fixed by the hole density δ through

$$\delta = \frac{1}{N} \sum_{\mathbf{k}} \int_{-\infty}^{+\infty} d\omega \rho(\omega + \mu, \mathbf{k}) n_{\text{F}}(\omega), \quad (13)$$

where $\rho(\omega, \mathbf{k})$ is the doping-independent hole spectral function (10), and $n_{\text{F}}(\omega)$ the Fermi function. For small hole doping ($\delta \ll Z_0$) the chemical potential lies in the coherent band and at zero temperature has a value $\mu = \pi\delta J / Z_0$.

Eqs. (6), (8), (9), and (13) completely describe the interaction between hole quasiparticles and spin waves in the impurity-free host and have been used in Ref. 3 to investigate the destruction of magnetism in weakly doped cuprates.

IV. THE EFFECT OF IMPURITIES

In this section we extend the theory to account for a finite density of nonmagnetic impurities in the system. As discussed in Sec. I B, we assume that the vacancies primarily act as pointlike potential scatterers for the mobile holes. Neglecting interference effects between spin-wave and impurity scattering processes for holes, we can capture the scattering off the impurities using a self-consistent T -matrix approach for the *dressed* hole quasiparticles, Eq. (10).

A. Scattering potential

Before proceeding a brief discussion of the quantum chemistry aspects is in order. Remarkably, there is no consensus on the description of Zn impurities within a one-band model for the CuO planes. Zn has a closed $3d^{10}$ configura-

tion, suggesting that holes are expelled.⁴⁵ This seems to be in agreement with cluster calculations in Ref. 46, which find the environment of a Zn atom to be similar to an undoped parent material. However, recent LDA calculations⁴⁷ have predicted a potential on the Zn site being repulsive for electrons (i.e., attractive for holes). In any case, the impurity potential is likely strong compared to the electron hopping. In what follows we will model Zn as repulsive pointlike scatterer for holes. For some parameter values we have also performed calculations with an attractive potential; the results will be mentioned below. (We note that Ref. 32 assumed a strongly attractive potential for holes associated to Li impurities in $\text{La}_2\text{Cu}_{1-y}\text{Li}_y\text{O}_4$; if this is correct, and the potential of Zn is repulsive for holes, this would provide a reasonable explanation for the different properties of $\text{La}_2\text{Cu}_{1-y}\text{Li}_y\text{O}_4$ and $\text{La}_{2-x}\text{Sr}_x\text{Cu}_{1-z}\text{Zn}_z\text{O}_4$.)

In our calculations, we will neglect the effect of the impurities on the spin waves. This piece of physics is well studied:^{9,10} the magnetism is suppressed rather slowly with vacancy doping (compared to hole doping). In principle, spin-wave scattering off the impurities could be taken into account along the lines of Ref. 9. In Sec. VI B we will account for this dilution/percolation effect by simply multiplying our results with a magnetization reduction factor taken from the studies of the diluted quantum Heisenberg antiferromagnet.

Further, we will also neglect the physics of impurity-induced moments.¹⁶⁻²⁰ We believe that magnetism arising from these moments alone is too weak to explain the large observed Néel temperatures, i.e., true bulk magnetism is required. In a bulk-ordered phase, the effective impurity moments will order below T_N due to the mean field arising from the bulk order parameter; this has been nicely seen⁴⁸ in $\text{La}_{2-x}\text{Sr}_x\text{Cu}_{1-z}\text{Zn}_z\text{O}_4$. However, the contribution of the impurity moments to the total order parameter is small.

B. Self-consistent T -matrix approach

For small impurity concentration, $n_{\text{imp}} \ll 1$, interference effects between different impurities are negligible, and the self-consistent T -matrix approximation⁴⁹ (SCTMA) is suitable to account for multiple scattering on a single impurity. Here we employ the SCTMA for spin-polaron quasiparticles, i.e., for holes which are already dressed by the interaction with spin waves. Within SCTMA the full-hole Green's function $\tilde{\mathcal{G}}(i\nu_n, \mathbf{k})$ is given by

$$\tilde{\mathcal{G}}^{-1}(i\nu_n, \mathbf{k}) = \mathcal{G}^{-1}(i\nu_n, \mathbf{k}) - \tilde{\Sigma}(i\nu_n, \mathbf{k}), \quad (14)$$

where $\mathcal{G}(i\nu_n, \mathbf{k})$ is the hole Green's function corresponding to the spectral density (10), and the hole self-energy from impurity scattering is

$$\tilde{\Sigma}(i\nu_n, \mathbf{k}) = n_{\text{imp}} T_{\mathbf{k}, \mathbf{k}}(i\nu_n). \quad (15)$$

For pointlike scatterers of strength V_0 , the T -matrix depends only on frequency as follows:

$$T_{\mathbf{k}, \mathbf{k}'}(i\nu_n) \equiv T(i\nu_n) = \frac{V_0}{1 - V_0 \tilde{\mathcal{G}}(i\nu_n)}, \quad (16)$$

and $\tilde{\mathcal{G}}(i\nu_n) = N^{-1} \sum_{\mathbf{k}} \tilde{\mathcal{G}}(i\nu_n, \mathbf{k})$ is the local hole Green's function.

With the replacements $\mathcal{G} \rightarrow \tilde{\mathcal{G}}$ (14) in Eqs. (8) and (9) and $\rho \rightarrow \tilde{\rho} = -\text{Im} \tilde{\mathcal{G}}/\pi$ in (13) we can now calculate how the impurities affect the spin-wave spectrum and consequently the magnetic properties of the AF host. In contrast to Ref. 2 we will not employ any further approximations.

V. MAGNETIC PROPERTIES

The spin-wave Green's functions defined in Sec. III allow for a direct calculation of static magnetic properties.

A. Staggered magnetization

The staggered magnetization in the Néel state decreases with hole doping,

$$m(\delta) = m_0 - \Delta m(\delta), \quad (17)$$

where the first term denotes the staggered moment in 2D AF reduced by ground-state spin-wave fluctuations only,

$$m_0 = \frac{1}{2} - \frac{1}{2N} \sum_{\mathbf{q}} \left(\frac{1}{\kappa_{\mathbf{q}}} - 1 \right), \quad (18)$$

with $\kappa_{\mathbf{q}} = (1 - \gamma_{\mathbf{q}}^2)^{1/2}$. For a square lattice and spin- $\frac{1}{2}$ we have the well-known spin-wave result $m_0 \approx 0.303$ (which is in excellent agreement with $m_0 = 0.3070(3)$ from quantum Monte Carlo simulations⁵⁰). The effect of doped holes on the AF order is included through the second term in (17), given by³⁵

$$\Delta m(\delta) = \frac{1}{N} \sum_{\mathbf{q}} \frac{\langle \alpha_{\mathbf{q}}^\dagger \alpha_{\mathbf{q}} \rangle - \gamma_{\mathbf{q}} \langle \alpha_{\mathbf{q}} \beta_{-\mathbf{q}} \rangle}{\kappa_{\mathbf{q}}}. \quad (19)$$

The bosonic occupation numbers in (19), being zero in the undoped case at $T=0$, can be calculated from the spin-wave Green's functions as $\langle \alpha_{\mathbf{q}}^\dagger \alpha_{\mathbf{q}} \rangle = -\mathcal{D}_{11}(\tau=0^-, \mathbf{q})$, $\langle \alpha_{\mathbf{q}} \beta_{-\mathbf{q}} \rangle = -\mathcal{D}_{21}(\tau=0^-, \mathbf{q})$. The phase boundary of the antiferromagnetic phase is given by $m(\delta_c) = 0$.

Notice that $m(\delta)$ (17) refers to the magnetization per spin (within the spin-wave approximation). To obtain the magnetization per site, as measured by bulk probes, $m(\delta)$ has to be multiplied with the factor $(1 - \delta - n_{\text{imp}})$; this does not change the location of the phase boundary, δ_c . Of course, this mean-field factor only crudely accounts for the dilution of the magnetic lattice; in particular, percolation physics cannot be captured. We will comment on this in Sec. VI B 2 below.

B. Néel temperature

The above calculations, performed at finite temperature, allow to determine the Néel temperature, T_N , from $m(\delta, T=T_N) = 0$. This requires a weak AF coupling, J_{\perp} , along the direction perpendicular to the CuO plane. In high- T_c cuprates this interlayer AF coupling is typically

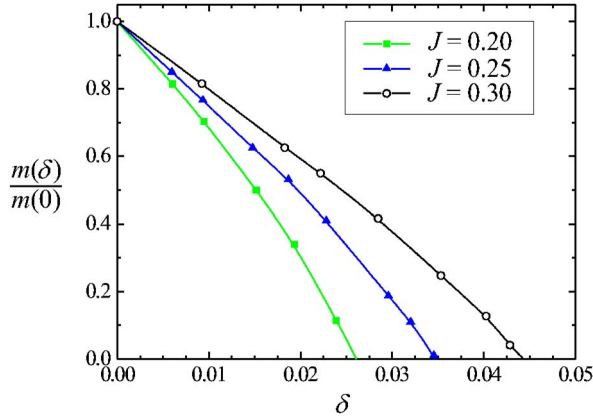


FIG. 1. (Color online) Doping dependence of the staggered magnetization for “mobile” (i.e., dispersive) holes (in the absence of impurities) for different values of J at $T=0$. (Typical parameters for cuprates obey $t/J=3-5$.) The weight of the dispersive quasiparticle peak in the hole spectrum is $Z_0=0.5J/t$; the lines are guides to the eye only. The data are very similar to the ones of Ref. 3.

$J_{\perp} \sim (10^{-5} - 10^{-4})J$. As a consequence, the spin-wave dispersion has a quasi-2D form which is given by

$$\tilde{\omega}_{\mathbf{q}}^0 = \frac{zJ}{2} \sqrt{\tilde{\gamma}_0^2 - \tilde{\gamma}_{\mathbf{q}}^2}, \quad (20)$$

where

$$\tilde{\gamma}_{\mathbf{q}} = \gamma_{\mathbf{q}} + \epsilon \gamma_{\mathbf{q}}^{\perp}. \quad (21)$$

Here $\gamma_{\mathbf{q}}^{\perp} = \cos q_z$, and the ratio between inter- and intralayer coupling is denoted by $\epsilon = J_{\perp}/(2J)$.

A drawback of the spin-wave approach is that no sensible critical behavior is obtained, i.e., the magnetization vanishes linearly as $T \rightarrow T_N$ (the order parameter critical exponent is $\beta=1$).

VI. NUMERICAL RESULTS

In this section we will present our numerical results for the doping dependence of the AF order parameter with and without impurities. Note that all energies are given in units of t . Most calculations are done for a two-dimensional system at zero temperature;⁵¹ the finite-temperature results are obtained using a finite interlayer coupling.

A. Hole-doped antiferromagnet without impurities

First we will discuss the case of the doped AF host without impurities and compare our results with published ones.^{2,3} Extending these calculations, we will consider different forms of the hole spectrum to study the influence of both hole dispersion and hole coherence on the host magnetism.

1. “Mobile” holes

The situation of “mobile” holes refers to a hole spectrum function as obtained from solving the single-hole problem in the t - J model, i.e., the hole spectral function consists of both a coherent, dispersive (11) and an incoherent, localized (12)

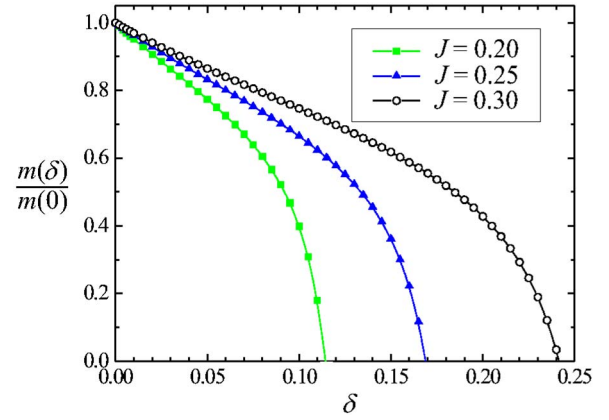


FIG. 2. (Color online) Doping dependence of the staggered magnetization now for “localized” holes, i.e., in the absence of a coherent quasiparticle peak in the hole spectrum ($Z_0=0$). The calculations have been done at temperature $T=0.005$, for fixed $J_{\perp}=0.01J$.

part. In Fig. 1 the zero-temperature doping dependence of the staggered magnetization is shown for different values of the coupling J and fixed quasiparticle weight Z_0 (taken from a single-impurity calculation^{36,39,40}).

For $J=0.2$ we obtain the similar critical hole concentration as Belkasri and Richard,³ $\delta_c \approx 2.7\%$. Our result for $J=0.25$ is a bit smaller than one derived by Khaliullin and Horsch,² $\delta_c \approx 4\%$, due to the fact that (as a further approximation) they have taken into account only the spin-wave self-energies with small momenta. The disappearance of the AF order at hole concentrations δ_c of a few percent is in good agreement with experiments on both $\text{La}_{2-x}\text{Sr}_x\text{CuO}_4$ and $\text{YBa}_2\text{Cu}_3\text{O}_{6+\delta}$.

2. “Localized” (incoherent) holes

Now we turn to a limiting case where the holes are localized in a certain extended region and only move incoherently (e.g., around a pinning center). With the above form of the spectral function (10) this corresponds to the quasiparticle weight being zero, $Z_0=0$. Thus, we use $\rho(\omega, \mathbf{k}) = \rho_{\text{incoh}}(\omega)$ (12). We study this toy situation to illustrate the strong influence of hole localization on the magnetic properties.

One expects the incoherent motion of holes is less destructive for the AF host in comparison with the case of “mobile” holes. In Fig. 2 we show the doping dependence of the staggered magnetization for “localized” holes and different values of AF coupling J . (t/J is still a relevant parameter here because the bandwidth of the incoherent motion is controlled by t . Also note that results are shown for finite temperatures and finite coupling J_{\perp} implying, e.g., that the value of the staggered magnetization $m(0)$ differs from the $T=0$ value m_0 . However, this difference is rather small since the effects of $T>0$ and $J_{\perp}>0$ tend to compensate.) The critical hole concentrations δ_c here are significantly larger than for dispersive holes, but still much smaller than for strictly static vacancies (where δ_c equals the percolation threshold $z_p=40.5\%$). The reason is of course that even our spatially localized holes scramble the magnetic background in their

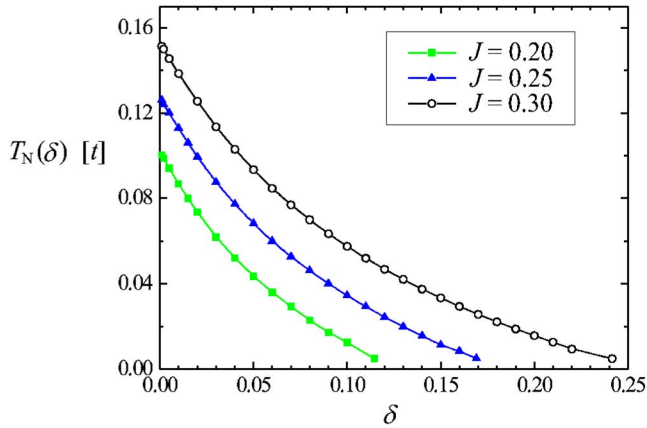


FIG. 3. (Color online) Doping dependence of the Néel temperature for “localized” holes ($Z_0=0$), with fixed $J_{\perp}=0.01J$. (Typical T_N values for undoped cuprates are a few hundred kelvins, e.g., La_2CuO_4 has $T_N \approx 300$ K. The hopping integral t in the t - J model for cuprates is 300–400 meV \approx 3000–4000 K.)

vicinity. We call the reader’s attention to the analysis of hole mobilities in Ref. 12, which concluded that “completely localized” holes (i.e., with zero mobility) still destroy the host magnetism three times faster than static vacancies; this gives $\delta_c \approx 13\%$ in reasonable agreement with our data in Fig. 2.

In Fig. 3 the doping dependence of the Néel temperature, T_N , for the “localized” holes is depicted for the same set of parameters as in Fig. 2. As also known for the case of doping with mobile holes,^{3,4} the initial suppression of the Néel temperature with doping is larger than the one of the staggered magnetization.

Comparing the results for “mobile” and “localized” holes, Figs. , one can easily conclude that incoherent motion of holes is less destructive than coherent motion. Therefore, any mechanism which modifies the hole spectral function in such a way that suppresses coherent and enhances incoherent motion will lead to a reinforcement of commensurate antiferromagnetism. (Note that the limit $t \rightarrow 0$, corresponding to immobile holes and percolative destruction of magnetism, is not described within the current approximation, but can be captured as in Sec. VI B 2 below.)

B. Hole-doped antiferromagnet with nonmagnetic impurities

Let us finally turn to our main results, namely the magnetic properties of the system with simultaneous hole and impurity doping. Here, the spin-wave properties are calculated using a hole spectrum function corresponding to “mobile” holes, i.e., consisting of a quasiparticle peak and an incoherent background, but subjected to impurity scattering (which redistributes weight in the hole spectrum).

Typical results for the AF order parameter as function of the hole doping are shown in Fig. 4. Clearly, Zn doping increases the critical hole concentration δ_c . The difference between the δ_c in a case with and without impurities is of order of 1% which is in reasonable agreement with experiments;¹² this indicates that we indeed capture the main effect of Zn doping in $\text{La}_{2-x}\text{Sr}_x\text{CuO}_4$. Notice that δ_c increases only weakly as function of the scattering potential V_0 for

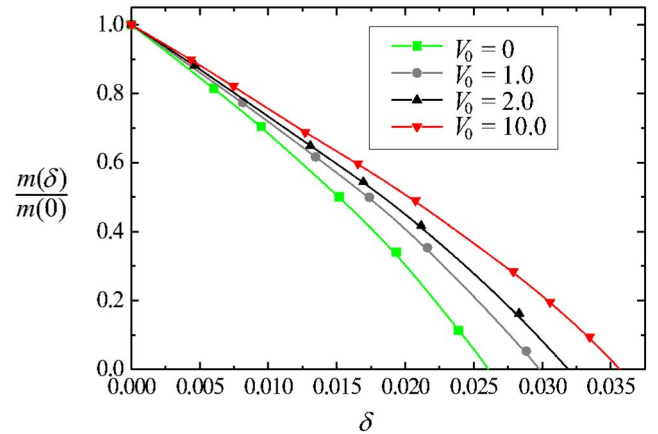


FIG. 4. (Color online) Doping dependence of the staggered magnetization for simultaneous hole and impurity doping. The different curves correspond to different impurity strengths V_0 , the impurity concentration is $n_{\text{imp}}=15\%$, the $V_0=0$ curve is the impurity-free case. The other parameters are $J=0.2$ and $Z_0=0.5J/t$, $T=0$.

$V_0 > 4$. We have performed calculations for different values of J , with qualitatively similar results (all δ_c values increase for larger J , see Fig. 1). In addition, we found that small to moderate negative V_0 has qualitatively the same effect as positive V_0 (strong negative V_0 leads to hole-bound states, where holes get trapped, and consequently a larger increase of δ_c through impurity doping).

1. Less coherent holes

Within our calculations we can clearly identify the reason for the antiferromagnetism being more robust in the presence of impurities. In the self-consistent T -matrix approach of Sec. IV the main effect of the impurity scattering is to transfer spectral weight, i.e., to reduce the weight of the coherent dispersive quasiparticle peak. We can quantify that: for $n_{\text{imp}}=15\%$ and $V_0=2$ the quasiparticle weight Z_0 is reduced by roughly 10%. A toy calculation with this reduced weight (but in the absence of impurities) shows that this loss of quasiparticle weight accounts for $\frac{3}{4}$ of the change in m between the clean and impurity-doped cases. (The remaining $\frac{1}{4}$ arises from a change in the quasiparticle dispersion and from reshuffling spectral weight at higher energies.)

Thus, the loss of coherence of the hole quasiparticle due to impurity scattering is the main source of the reinforcement of magnetism. We can interpret this in real space: The coherent motion of the hole quasiparticle in the antiferromagnetic background corresponds to the emission of a spin wave in each hopping step, with a strong suppression of the order parameter. In contrast, during the incoherent motion within the quasiparticle the hole also absorbs spin waves (due to self-retracing paths), and the suppression of antiferromagnetism is less severe.

2. Spin-wave scattering and percolation

Our approach has so far neglected the dilution effect of the vacancies on the magnetic, i.e., spin-wave, part of the model. On the mean-field level, dilution results in a multipli-

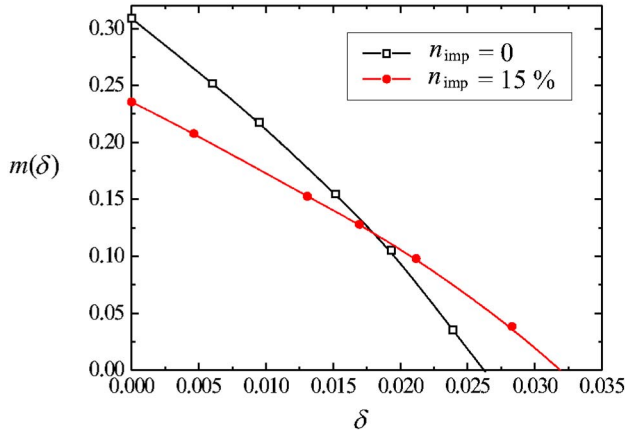


FIG. 5. (Color online) Reappearance of the AF ordering through impurities: The staggered magnetization, corrected by the percolation factor $P(n_{\text{imp}})$ (see text), as function of hole doping for zero and 15% impurity concentration. The parameters are $J=0.2$, quasiparticle weight $Z_0=0.5J/t$, impurity potential $V_0=2$, $T=0$.

cative factor of $(1-\delta-n_{\text{imp}})$ for m to obtain the staggered magnetization per site. However, impurity scattering of spin waves is still not included, and our approach falls short of capturing percolation physics. While the impurity effect on spin waves could be treated in principle,⁹ we choose a different route here: As dilution of a well-ordered antiferromagnet has been studied extensively,¹⁰ we can simply multiply our magnetization results with a renormalization factor $P(n_{\text{imp}})$ which represents the (normalized) magnetization of a 2D square lattice quantum Heisenberg magnet diluted with n_{imp} vacancies; this quantity can be taken from quantum Monte Carlo simulations, Fig. 18 of Ref. 10. With this we reproduce a vanishing magnetization at the percolation threshold.¹⁴

3. Reappearance of magnetism

To emphasize the fact that impurities help the AF order to recover we show in Fig. 5 the staggered magnetization m at zero temperature as a function of hole doping with and without impurities; here m is *not* normalized to its value at $\delta=0$. Another way to show the recovery of long-range order in the presence of impurities is presented in Fig. 6, where order parameter is plotted as a function of impurity concentration for two different hole dopings. For $\delta=2.7\%$ the AF order sets in at finite impurity concentration, $n_{\text{imp}} \approx 2.5\%$. The presence of impurities causes the reappearance of the AF order for hole concentrations greater than $\delta \approx 2.6\%$, and the order parameter depends nonmonotonically on the hole doping; both results are in good agreement with the experiments done on $\text{La}_{2-x}\text{Sr}_x\text{Cu}_{1-z}\text{Zn}_z\text{O}_4$ by Hücker *et al.*¹²

For a detailed comparison with experiments a few remarks are in order: (i) The present calculation is strictly valid only for small impurity concentration, $n_{\text{imp}} \ll 1$, when the interaction between impurities is negligible. (ii) Our simplified treatment of magnetic dilution, utilizing numerical results for the diluted insulating Heisenberg antiferromagnet, only partially captures the interplay of dilution and quantum fluctuations. In particular, in the presence of vacancies and a small

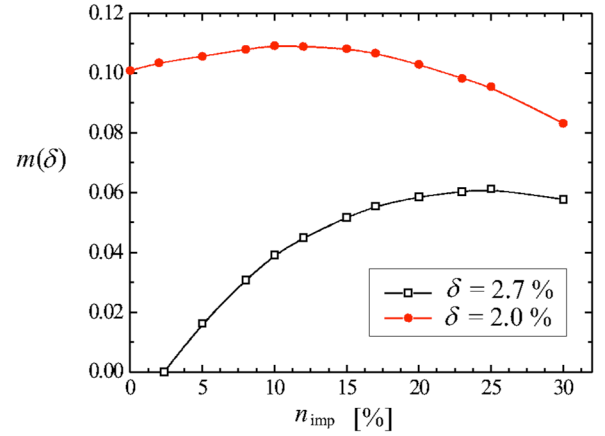


FIG. 6. (Color online) Same as Fig. 5, but now showing m as function of the impurity concentration for different fixed hole dopings. m vanishes at the percolation threshold, $n_{\text{imp}}=40.5\%$.

amount of holes magnetic order does not need to persist up to the percolation threshold.¹⁴ Thus, our data at finite hole doping become unreliable for $n_{\text{imp}} > 25\%$. (iii) Corrections beyond spin-wave theory are required for the description of critical behavior in the vicinity of δ_c ; we expect m to vanish with an infinite slope (i.e., the order parameter exponent β being smaller than unity). (iv) Experiments usually measure the ordering temperature T_N , not the zero-temperature order parameter m . Although the two behave in a qualitatively similar fashion, T_N decreases initially faster with doping than m . Also, for a complete picture it may be necessary to include the interlayer coupling beyond mean field.⁵² The detailed behavior of T_N with both hole and impurity doping, taking into account percolation-type physics, is beyond the scope of this paper.

In Fig. 7 we show the evolution of the critical hole doping level δ_c with the impurity concentration. Interestingly (and in agreement with experiment), the variation of δ_c is rather small, i.e., vacancies cannot be used to shift δ_c to arbitrarily large values.

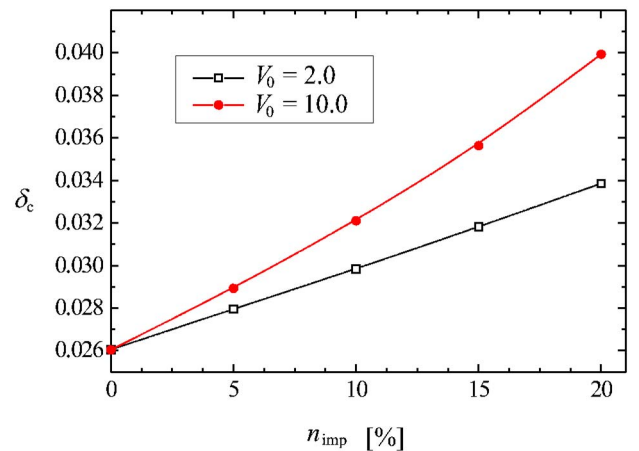


FIG. 7. (Color online) Critical hole doping level, δ_c , as function of the impurity concentration n_{imp} for different values of the scattering potential. The parameters are $J=0.2$, quasiparticle weight $Z_0=0.5J/t$, $T=0$.

Last but not least, we briefly comment on the calculation by Korenblit *et al.*,³³ which provides a different explanation for the experiments of Ref. 12. They present scaling arguments based on the frustration model, with the key idea that Zn removes ferromagnetic bonds created by hole doping. This simple theory predicts that δ_c can be increased to large values by introducing Zn impurities; this is in contradiction to the experiment. Thus, their simple scaling form $\delta \rightarrow \delta(1 - n_{\text{imp}})^2$ cannot apply to larger δ and n_{imp} . Also, the paper makes no reference to the motion and the mobility of holes, and we think that this aspect is crucial for the description of hole-doped cuprates.

VII. CONCLUSIONS

Motivated by experiments on Zn-doped $\text{La}_{2-x}\text{Sr}_x\text{CuO}_4$, we have discussed the interplay of mobile holes and static nonmagnetic impurities in lightly doped antiferromagnetic Mott insulators. Based on a self-consistent spin-wave and T -matrix calculations we have shown that commensurate long-range order is more robust against hole doping in the presence of nonmagnetic impurities as compared to the clean case.

We believe that the most naive picture, namely that Zn impurities trap holes, is not appropriate. This can already be seen from the experimental data: at a hole doping of 2.3% the Néel temperature depends strongly and nonmonotonically on the impurity concentration for $4\% < n_{\text{imp}} < 15\%$. Instead, we propose that impurities mainly reduce the hole mobility and suppress the coherent part of the hole motion (in favor of an incoherent background). In turn, this suppresses the spin-wave softening caused by coherent hole motion. In the case of Ni doping¹³ this effect is corroborated by the ordering tendencies of the spin-1 impurity moments.

ACKNOWLEDGMENTS

We are grateful to M. Hücker for numerous insightful discussions about the experiments on Zn-doped $\text{La}_{2-x}\text{Sr}_x\text{CuO}_4$, and for sharing unpublished results. We also thank H. Alloul, J. Brinckmann, C.-H. Chung, M. Indergand, S. Florens, and C. M. Varma for useful comments. This research was supported by the DFG Center for Functional Nanostructures and the Virtual Quantum Phase Transitions Institute (Karlsruhe), as well as NSF Grant No. PHY99-0794 (KITP Santa Barbara).

-
- ¹Ch. Niedermayer, C. Bernhard, T. Blasius, A. Golnik, A. Moodenbaugh, and J. I. Budnick, Phys. Rev. Lett. **80**, 3843 (1998).
²G. Khaliullin and P. Horsch, Phys. Rev. B **47**, 463 (1993).
³A. Belkasri and J. L. Richard, Phys. Rev. B **50**, 12896 (1994).
⁴J. L. Richard and V. Yu. Yushankhaï, Phys. Rev. B **50**, 12927 (1994).
⁵I. R. Pimentel, F. Carvalho Dias, L. M. Martelo, and R. Orbach, Phys. Rev. B **60**, 12329 (1999).
⁶A. Aharony, R. J. Birgeneau, A. Coniglio, M. A. Kastner, and H. E. Stanley, Phys. Rev. Lett. **60**, 1330 (1988).
⁷V. Cherepanov, I. Ya. Korenblit, A. Aharony, and O. Entin-Wohlman, Eur. Phys. J. B **8**, 511 (1999).
⁸Y.-C. Chen and A. H. Castro Neto, Phys. Rev. B **61**, R3772 (2000).
⁹A. L. Chernyshev, Y. C. Chen, and A. H. Castro Neto, Phys. Rev. Lett. **87**, 067209 (2001), Phys. Rev. B **65**, 104407 (2002).
¹⁰A. W. Sandvik, Phys. Rev. B **66**, 024418 (2002).
¹¹O. P. Vajk, P. K. Mang, M. Greven, P. M. Gehring, and J. W. Lynn, Science **295**, 1691 (2002).
¹²M. Hücker, V. Kataev, J. Pommer, J. Haraß, A. Hosni, C. Pflichtsch, R. Gross, and B. Büchner, Phys. Rev. B **59**, R725 (1999).
¹³T. Machi, I. Kato, R. Hareyama, N. Watanabe, Y. Itoh, N. Koshizuka, S. Arai, and M. Murakami, Physica C **388–389**, 233 (2003).
¹⁴If the ordered moment in an impurity-free magnet is already strongly reduced by quantum effects (e.g., in a bilayer system), then magnetic order can disappear upon dilution *before* the percolation threshold; see, e.g., Ref. 15.
¹⁵R. Sknepnek, T. Vojta, and M. Vojta, Phys. Rev. Lett. **93**, 097201 (2004); T. Vojta and J. Schmalian, *ibid.* **95**, 237206 (2005).
¹⁶G. B. Martins, M. Laukamp, J. Riera, and E. Dagotto, Phys. Rev. Lett. **78**, 3563 (1997).
¹⁷A. W. Sandvik, E. Dagotto, and D. J. Scalapino, Phys. Rev. B **56**, 11701 (1997).
¹⁸M. Vojta, C. Buragohain, and S. Sachdev, Phys. Rev. B **61**, 15152 (2000).
¹⁹C. Yasuda, S. Todo, M. Matsumoto, and H. Takayama, Phys. Rev. B **64**, 092405 (2001).
²⁰S. Wessel, B. Normand, M. Sigrist, and S. Haas, Phys. Rev. Lett. **86**, 1086 (2001).
²¹S. Sachdev and M. Vojta, in *Proceedings of the XIII International Congress on Mathematical Physics*, edited by A. Fokas (International Press, Boston, 2001).
²²J. Bobroff, W. A. MacFarlane, H. Alloul, P. Mendels, N. Blanchard, G. Collin, and J.-F. Marucco, Phys. Rev. Lett. **83**, 4381 (1999).
²³J. A. Hodges, Y. Sidis, P. Bourges, I. Mirebeau, M. Hennion, and X. Chaud, Phys. Rev. B **66**, 020501(R) (2002).
²⁴H. Kimura, M. Kofu, Y. Matsumoto, and K. Hirota, Phys. Rev. Lett. **91**, 067002 (2003); M. Kofu, H. Kimura and K. Hirota, cond-mat/0409747, Phys. Rev. B (to be published).
²⁵S. Wakimoto, R. J. Birgeneau, A. Kagedan, H. Kim, I. Swainson, K. Yamada, and H. Zhang, Phys. Rev. B **72**, 064521 (2005).
²⁶H.-H. Klauss, W. Wagener, B. Büchner, M. Hücker, D. Mienert, W. Kopmann, M. Birke, H. Luetkens, D. Baabe, and F. J. Litterst, Hyperfine Interact. **133**, 203 (2001).
²⁷In lightly hole-doped $\text{YBa}_2\text{Cu}_3\text{O}_{6+\delta}$ it was found that Zn codoping *weakens* ordered magnetism; see H. Alloul, P. Mendels, H. Casalta, J. F. Marucco, and J. Arabski, Phys. Rev. Lett. **67**, 3140 (1991). This is in contrast to the results on $\text{La}_{2-x}\text{Sr}_x\text{Cu}_{1-z}\text{Zn}_z\text{O}_4$.¹² While we have no conclusive theoretical picture, we speculate that this difference is due to the presence of CuO chains in $\text{YBa}_2\text{Cu}_3\text{O}_{6+\delta}$. The locations of both holes and Zn as function of δ and z are not known.

- ²⁸A. Oosawa, T. Ono, and H. Tanaka, *Phys. Rev. B* **66**, 020405(R) (2002).
- ²⁹M. Hücker, H.-H. Klauss, A. Hosni, and B. Büchner (unpublished).
- ³⁰B. J. Suh, P. C. Hammel, Y. Yoshinari, J. D. Thompson, J. L. Sarrao, and Z. Fisk, *Phys. Rev. Lett.* **81**, 2791 (1998).
- ³¹T. Park, Z. Nussinov, K. R. A. Hazzard, V. A. Sidorov, A. V. Balatsky, J. L. Sarrao, S.-W. Cheong, M. F. Hundley, J.-S. Lee, Q. X. Jia, and J. D. Thompson, *Phys. Rev. Lett.* **94**, 017002 (2005); Y. Chen, W. Bao, Y. Qiu, J. E. Lorenzo, J. L. Sarrao, D. L. Ho and M. Y. Lin, *Phys. Rev. B* **72**, 184401 (2005).
- ³²O. P. Sushkov and A. H. Castro Neto, cond-mat/0504234 (unpublished).
- ³³I. Ya. Korenblit, A. Aharony, and O. Entin-Wohlman, *Phys. Rev. B* **60**, R15017 (1999).
- ³⁴C. Buhler, S. Yunoki, and A. Moreo, *Phys. Rev. B* **62**, R3620 (2000).
- ³⁵Our derivation is closest to the one of Ref. 3, but the equations for the chemical potential and the magnetization correction differ by factors of 2.
- ³⁶C. L. Kane, P. A. Lee, and N. Read, *Phys. Rev. B* **39**, 6880 (1989).
- ³⁷J. I. Igarashi and P. Fulde, *Phys. Rev. B* **45**, 12357 (1992).
- ³⁸A. Sherman and M. Schreiber, *Phys. Rev. B* **48**, 7492 (1993), *Phys. Rev. B* **50**, 12887 (1994).
- ³⁹S. Schmitt-Rink, C. M. Varma, and A. E. Ruckenstein, *Phys. Rev. Lett.* **60**, 2793 (1988).
- ⁴⁰G. Martínez and P. Horsch, *Phys. Rev. B* **44**, 317 (1991).
- ⁴¹E. Dagotto, *Rev. Mod. Phys.* **66**, 763 (1994); Yu. A. Izyumov, *Phys. Usp.* **40**, 445 (1997).
- ⁴²B. O. Wells, Z.-X. Shen, A. Matsuura, D. M. King, M. A. Kastner, M. Greven, and R. J. Birgeneau, *Phys. Rev. Lett.* **74**, 964 (1995).
- ⁴³A. Nazarenko, K. J. E. Vos, S. Haas, E. Dagotto, and R. J. Gooding, *Phys. Rev. B* **51**, R8676 (1995); P. W. Leung, B. O. Wells, and R. J. Gooding, *ibid.* **56**, 6320 (1997); A. V. Chubukov, and D. K. Morr, *ibid.* **57**, 5298 (1998).
- ⁴⁴C. Kim, P. J. White, Z.-X. Shen, T. Tohyama, Y. Shibata, S. Maekawa, B. O. Wells, Y. J. Kim, R. J. Birgeneau, and M. A. Kastner, *Phys. Rev. Lett.* **80**, 4245 (1998).
- ⁴⁵A. V. Balatsky, I. Vekhter, and J.-X. Zhu, cond-mat/0411318, *Rev. Mod. Phys.* (to be published).
- ⁴⁶C. Bersier, S. Renold, E. P. Stoll, and P. F. Meier, cond-mat/0504562 (unpublished).
- ⁴⁷L.-L. Wang, P. J. Hirschfeld, and H.-P. Cheng, cond-mat/0505014, *Phys. Rev. B* (to be published).
- ⁴⁸M. Hücker and B. Büchner, *Phys. Rev. B* **65**, 214408 (2002).
- ⁴⁹P. J. Hirschfeld, P. Wölfle, and D. Einzel, *Phys. Rev. B* **37**, 83 (1988).
- ⁵⁰A. W. Sandvik, *Phys. Rev. B* **56**, 11678 (1997).
- ⁵¹The zero-temperature calculations have been done with an artificial broadening, $\eta=0.005$, of δ peaks in the propagators, to simplify the numerics.
- ⁵²M. Hücker, H.-H. Klauss, and B. Büchner, *Phys. Rev. B* **70**, 220507(R) (2004).